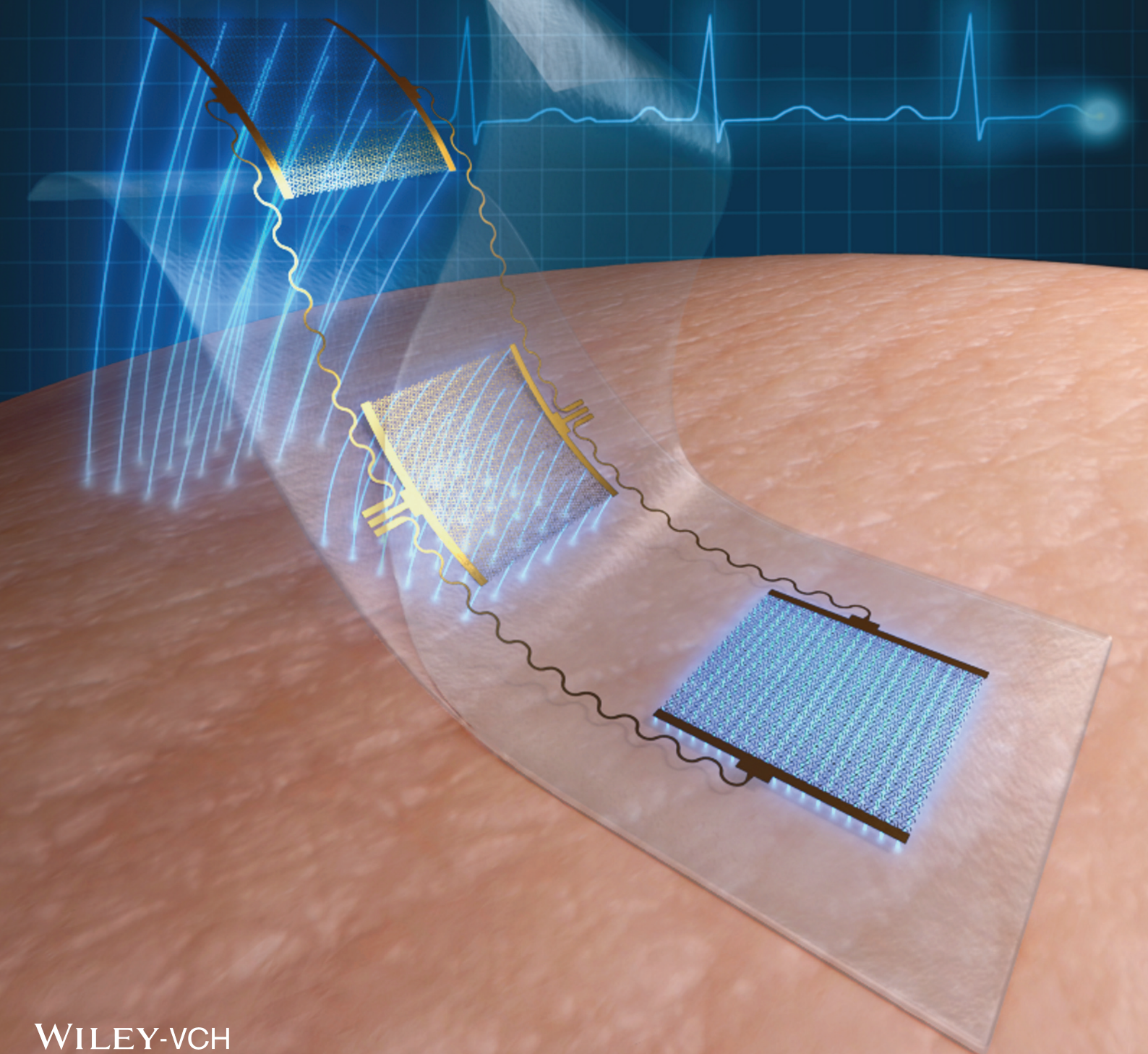


ADVANCED HEALTHCARE MATERIALS



Capacitive Epidermal Electronics for Electrically Safe, Long-Term Electrophysiological Measurements

Jae-Woong Jeong, Min Ku Kim, Huanyu Cheng, Woon-Hong Yeo, Xian Huang, Yuhao Liu, Yihui Zhang, Yonggang Huang, and John A. Rogers*

Capacitive sensing of electrophysiological (EP) signals involves measurements of electrical coupling between biological tissues and electrodes, mediated by an intervening dielectric layer. Using this approach, electrocardiograms (ECGs), electromyograms (EMGs), electrooculograms (EOGs), and other EP signals can be recorded in a manner that allows the electrode materials to be fully encapsulated and protected from the surroundings. Such features facilitate sterilization and enable cleaning for reuse; they also enhance safety by eliminating leakage currents and electrical shorts between the devices and the biology. For use on the skin, this design also avoids irritation and allergic reactions that can be caused by electrolyte gels^[1] or by direct contact of metal electrodes.^[2,3] Past work demonstrated capacitive sensors that combine flat, rigid electrodes or conductive fabrics with various insulators such as pyre varnish,^[4] silicone dioxide,^[5] polydimethylsiloxane (PDMS),^[6] or cloth.^[7] Although such electrodes can be fixed by caps, belts, or tapes to the skin,^[8,9] conformal contact

can be difficult to guarantee. As a result, acquired signals can be susceptible to artifacts associated with motion-induced changes in the coupling capacitance. In addition, the relatively thick, bulk nature of these electrodes can lead to inconvenient form factors, limited options in mounting locations, and discomfort in long-term usage.

Previously, deformable capacitors were demonstrated as sensors^[10–13] for measuring pressure or strain. Approaches to capacitive sensing of EP are possible by using the principles of epidermal electronic systems (EES),^[14] in which key physical properties of the devices—area mass density, thickness, and effective mechanical modulus—are designed to match those of the epidermis. Here, integrated electronics and sensors take the form of thin, stretchable membranes that can be integrated with the skin in a way that yields intimate, conformal contact at the electrode–skin interface by van der Waals interactions alone. Addition of capacitive sensing capabilities in EES structures offers an opportunity to enhance the robustness in operation for EP measurement over both conventional capacitive approaches and previously demonstrated direct contact EES electrodes. This paper introduces capacitive EES designs that are reusable, electrically safe, and minimally sensitive to motion artifacts. Demonstration experiments on human subjects illustrate levels of fidelity in ECG, EMG, and EOG recordings that are comparable to those of standard gel electrodes and of direct contact EES electrodes.

Figure 1a shows an example of capacitive EES electrodes for measurement, ground, and reference coupled to the skin through a soft, elastomeric insulating layer. The sensing mechanism relies on displacement currents ($J_d = \epsilon_r \epsilon_0 \frac{dE(t)}{dt}$; ϵ_r : relative permittivity of the material, ϵ_0 : vacuum permittivity, and $E(t)$: time-varying electric field) induced in electrodes that lie in proximity to the skin. The resulting signals are captured as voltages measured using a pre-amplifier with high input impedance. In this manner, EP recordings occur indirectly without direct electrode contact or charge transport.

Capacitive sensors in the EES design (Figure 1b) can naturally achieve conformal contact against the soft, rough, and irregular surfaces of the skin. The low modulus, elastic mechanics of the device also avoids any constraints on natural motions of the skin. The construction relies on three gold electrodes (200 nm in thickness) insulated with silicone, associated interconnect wires, and an anisotropic conductive film (ACF; Elform, USA) that connects to peripheral bonding pads for external data acquisition. To afford the desired soft mechanics, the electrodes exploit filamentary serpentine (FS) mesh layouts (30 μm in width) as shown in Figure 1c, and reported previously. The interconnect metal is encapsulated

Dr. J.-W. Jeong, Dr. W.-H. Yeo, Dr. X. Huang, Y. Liu
Department of Materials Science and Engineering
Beckman Institute for Advanced Science and
Technology, and Frederick Seitz Materials Research
Laboratory
University of Illinois at Urbana-Champaign
Urbana, IL 61801, USA



M. K. Kim
Department of Electrical and Computer Engineering
University of Illinois at Urbana-Champaign
Urbana, IL 61801, USA

H. Cheng, Dr. Y. Zhang, Prof. Y. Huang
Department of Civil and Environmental Engineering
Department of Mechanical Engineering
Northwestern University
Evanston, IL 60208, USA

H. Cheng, Prof. Y. Huang
Center for Engineering and Health Skin Disease Research Center
Northwestern University
Evanston, IL 60208, USA

Dr. Y. Zhang
Center for Mechanics and Materials
Tsinghua University
Beijing 100084, China

Prof. J. A. Rogers
Department of Materials Science and Engineering
Beckman Institute for Advanced Science and Technology
and Frederick Seitz Materials Research Laboratory
University of Illinois at Urbana-Champaign
Urbana, IL 61801, USA
E-mail: jrogers@illinois.edu

DOI: 10.1002/adhm.201300334

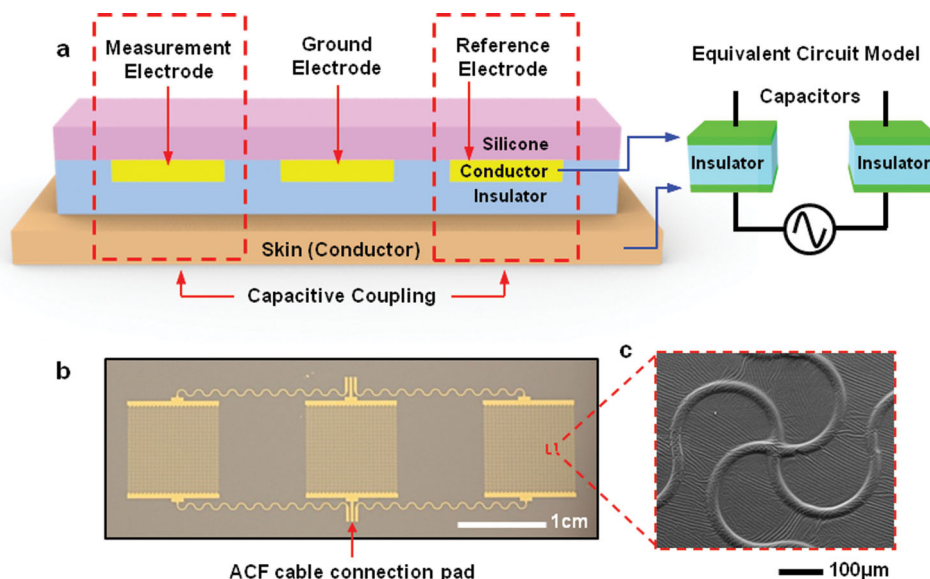


Figure 1. Schematic illustration of an epidermal electronic system (EES) with a capacitive sensor for electrophysiological (EP) measurement using insulated electrodes for measurement, ground and reference. a) Capacitive EES on the skin and an equivalent circuit model. Capacitive coupling through the insulation layer provides the basis for detecting EP signals. b) Optical image of a capacitive EES, c) Scanning electron image of a unit cell of the filamentary serpentine (FS) mesh electrode structure. The filaments, which consist of thin metal films encapsulated above and below by coatings of polyimide, have widths of 30 μm and total thickness of <1 μm .

between layers of polyimide (PI; 300 nm in thickness, Sigma-Aldrich, USA) on top and bottom, thereby positioning the metal at the neutral mechanical plane (NMP) of the structure. This layout minimizes bending stresses in the active materials. The contact pads are exposed to allow bonding to ACF, which connects the capacitive sensor to the measurement circuit for signal acquisition. According to finite element analysis of the mechanics, stretching the structure to tensile strains of $\approx 30\%$ (the limit of elastic deformation of the skin^[15] induces maximum principal strains of only 0.8% in the metals (fracture strain of Au $\approx 1\%$) (Figure S1, Supporting Information).

The processes for fabricating a capacitive EES and applying it onto the skin appear in Figure S2 (Supporting Information). The Experimental Section provides the details. A thin silicone substrate (5 μm thickness; Solaris, Smooth-On, USA) coated on a water-soluble polymer sheet (polyvinyl alcohol (PVA), Haining Sprutop Chemical Tech, China) serves as a substrate. The latter provides a temporary support to allow manual mounting on the skin. Capacitive sensors in the EES design require a transparent, biocompatible insulating layer with high permittivity, large stretchability, and large adhesion force for strong signal coupling, accommodation of skin deformation, and robust lamination onto the skin, respectively. Table S1 (Supporting Information) compares properties of some commercially available transparent, biocompatible materials (PDMS, Solaris, and spray-on-bandage). Among these materials, Solaris (Smooth-On, USA) offers the most suitable set of properties: moderate relative permittivity (2.78), large adhesion force, low elastic modulus (98 kPa; 2:1 Solaris) and high elongation at break (290%). Further improvements in permittivity can be achieved, for example, by mixing high- k nanoparticles (e.g., BaTiO_3) into the silicone matrix.^[16] As demonstrated in the following,

even these pure silicone materials, in the thicknesses reported here, provide sufficient electrical coupling. After laminating the device onto the skin, the PVA sheet is removed by applying water, thereby leaving only the EES adhered conformally onto the skin by van der Waals interactions.

The external measurement system exploits an ultra-high input impedance voltage follower with amplifying and filtering circuitry (Figure 2a). In comparison to conventional direct-contact Ag/AgCl electrodes with coupling gels, the impedance between the skin and a capacitive electrode is high due to the presence of the insulating layer.^[17] As a result, a pre-amplifier with ultra-high input impedance must be used for signals acquisition with low loss. The gain of the pre-amplifier, which uses a voltage follower design, can be approximated as:

$$G(s) = \frac{V_{\text{out}}(s)}{V_{\text{in}}(s)} = \frac{s C_E R_B}{1 + s(C_E + C_{\text{in}}) R_B} \quad (1)$$

where C_E is the capacitance of an insulated electrode, R_B is a bias resistance between the ground and the input of the operational amplifier (op amp), R_{in} and C_{in} are the input resistance and capacitance of the op amp, respectively. A signal can be capacitively coupled with near unity gain when C_E is much larger than C_{in} . Our system uses an op amp with ultra-high input impedance and extremely low-input capacitance (OPA124, Texas Instruments, USA; Impedance = $10^{14} \Omega \parallel 3\text{pF}$). R_B helps to eliminate static charges that can potentially accumulate at the skin–electrode interface. Because the parallel connection of C_E to R_B forms a first-order high-pass filter, as indicated in Equation 1, the bias resistance ($R_B = 40 \text{ G}\Omega$) must be carefully chosen to yield a cutoff frequency ($f_c = \frac{1}{2\pi R_B C_E}$) outside of the operating frequency band.^[6]

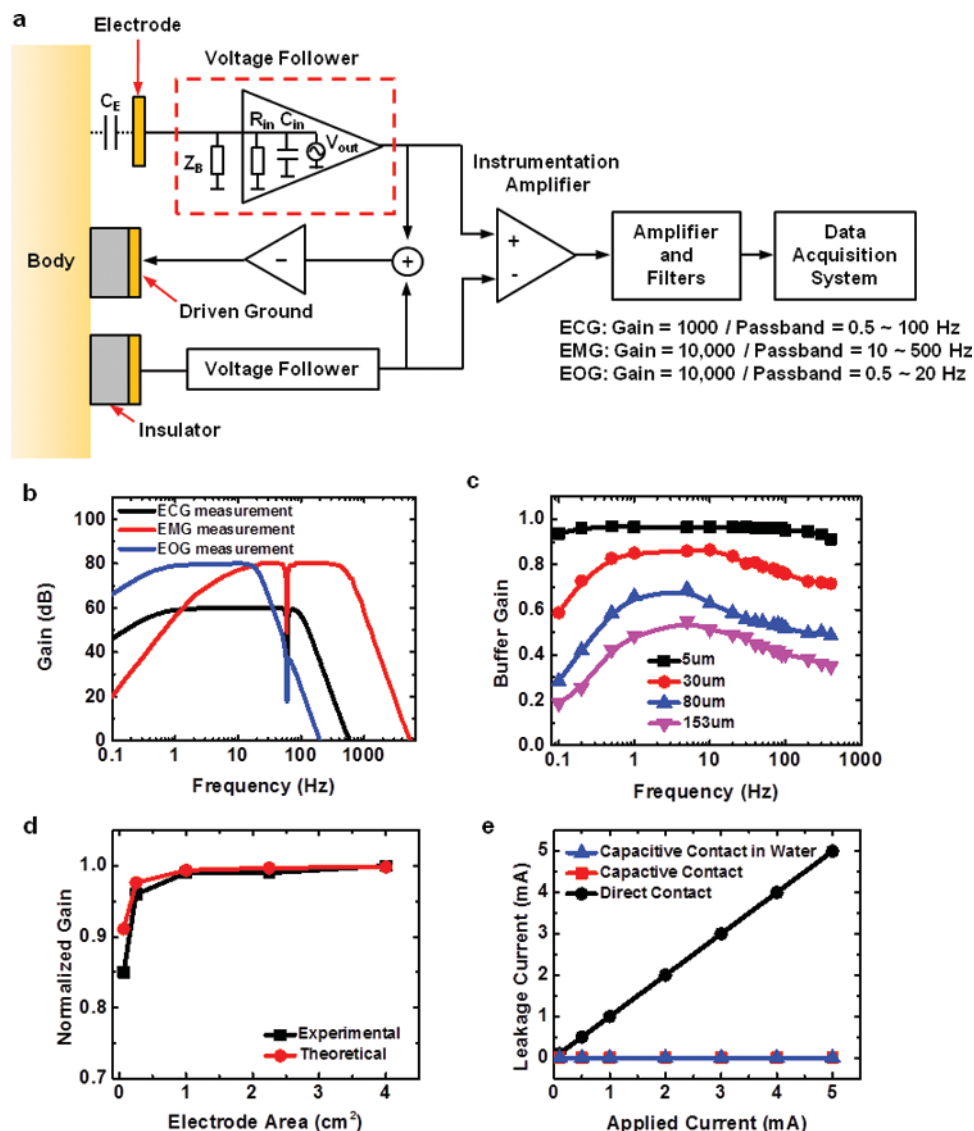


Figure 2. Design and characteristics of capacitive sensing system. a) Schematic diagram of the capacitive sensing system. Signals from the measurement and reference electrodes are amplified and filtered through a circuitry, and digitalized data are recorded in a computer. The driven ground provides negative feedback to eliminate common noise. b) Gain-frequency spectrum obtained in ECG, EMG, and EOG measurement modes. -3 dB cutoff frequency reading shows a passband of 0.5–100 Hz in ECG mode; 10–500 Hz in EMG mode; and 0.5–20 Hz in EOG mode. c) Plot of a pre-amplifier gain as a function of frequency for variant thicknesses of the insulation layer, d) Plot of gain dependence on the electrode area, e) Amount of leakage current through electrodes in various contact scenarios: 1) capacitive contact in water, 2) capacitive contact in ambient environment, 3) direct contact.

An instrumentation amplifier (AD620, Analog Devices, USA; common-mode rejection ratio = 100 dB) amplifies the potential difference between the measurement and the reference electrodes, to suppress common mode noise in each input signal. A driven ground (Figure S3, Supporting Information) provides negative feedback of the residual common-mode noise to the ground on the skin, thereby further improving the signal-to-noise ratio (SNR). The amplifier and filter unit provide tunable gain (60–80 dB) for ECG, EMG, and EOG measurements. The passband of the circuit can be digitally varied using LabVIEW software (National Instruments, USA). A 60-Hz notch filter eliminates power line interference. The acquired signals are digitized at a sampling rate of 1 kHz by

an analog-to-digital converter (NI USB-6363, National Instruments, USA) and displayed on a computer screen. A schematic diagram of the detailed circuit design and a printed circuit board embodiment appear in Figure S4 (Supporting Information). Figure 2b presents gain-frequency spectra measured in the ECG, EMG, and EOG measurement modes. The system provides a gain of 60 dB in the range of 0.5–100 Hz for ECG; and a gain of 80 dB in the range of 10–500 Hz and 0.5–20 Hz for EMG and EOG, respectively.

Capacitance between the skin and the insulated electrodes (C_E) determines the SNR through its effect on the gain of the pre-amplifier. The influence of electrode design on capacitive coupling is, therefore, important. Systematic studies based

on capacitive EES measurements of AC signals introduced onto metal substrates reveal the effects (Figure S5, Supporting Information). Figure 2c shows the pre-amplifier gain over a frequency range of 0.1–400 Hz for different insulation layer thicknesses on FS electrodes with sizes of 1 cm × 1 cm and areal coverages of 25%. The increase in gain at low frequencies (<2 Hz) results from the high-pass filter behavior of the pre-amplifier. Of the cases studied, capacitive electrodes with 5 μm-thick insulating layers exhibit the highest stable gain over the frequency range of interest, due primarily to their relatively high C_E (≈120 pF). As expected, the gain is also improved as the C_E is increased by increasing the sizes of the electrodes. Figure 2d shows effects of size from 0.5 cm × 0.5 cm to 4 cm × 4 cm, each with an areal coverage of 25%.

Thin insulating layers are preferred due to their ability to enhance conformal contact with the skin. Such contact is possible when the adhesion energy of the contact is larger than the sum of the bending energy associated with the EES and the elastic energy of deformation of the skin. According to an analytical mechanics model in which the skin surface morphology is assumed to be sinusoidal with a characteristic amplitude (55 μm) and wavelength (140 μm),^[18] the critical thickness (i.e., total effective thickness of the EES) for perfect conformal contact is ≈30 μm (Figure S7, Supporting Information) when the membrane consists of an insulating layer of Solaris (Young's modulus: 98 kPa) on top of a 5-μm-thick substrate layer of Solaris with the EES electrodes (plane-strain modulus of Au: 97 GPa, areal ratio of EES on the Solaris membrane: 25%). This critical thickness decreases with skin motion due to a new skin morphology that induces additional strain on the initially conformed EES/skin system. For the skin stretching up to 30%, however, the total critical thickness (resulted from both Solaris insulation layer and 5 μm-thick Solaris substrate layer) remains greater than 26 μm (Figure S8, Supporting Information). Supporting Information shows details of the interface mechanics between EES and the skin. An EES constructed with a 5-μm-thick layer of Solaris as an insulator (total thickness of the EES ≈ 10 μm) is well below this critical thickness. This design serves as the basis for device measurements described hereafter.

The capacitive design removes the possibility of electrical leakage from the electronics to the body and fluidic leakage from the body to the electronics. Electrical leakage can represent a health risk, even at relatively low levels, especially for patients with weakened immune systems. According to the general standard (IEC 60601–1) for medical electrical equipment,^[19] maximum leakage currents must be below 0.5 mA. Measurements (Figure 2e) show that a capacitive EES with FS electrodes that span an area of 1 cm × 1 cm with 25% coverage exhibit leakage currents below 10 nA when 5 mA passes through the structure, for both dry and wet conditions. Such properties ensure electrical safety not only for use on the skin but also for application on surfaces of internal organs such as the heart and the brain.

The insulation layer also serves as an effective encapsulant to prevent degradation of the electrodes, thereby facilitating sterilization and enabling cleaning operations for reuse. The results of Figure 3 demonstrate some of these features. Here, the EES (10 μm in total thickness), initially attached on the right forearm for EMG measurement, is retrieved using a water-soluble tape

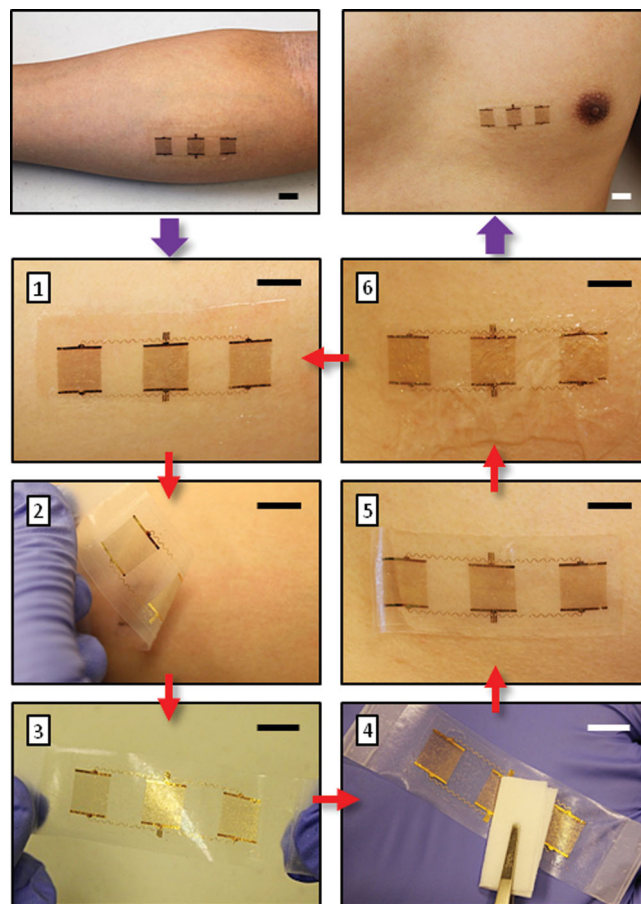


Figure 3. Demonstration of sterilization and recycling processes of a capacitive EES. The scale bar indicates 1 cm. The device initially on the right forearm for EMG measurement is moved to the left chest for acquisition of ECG signals through a process as follows: 1) Capacitive EES on the forearm ready for retrieval, 2) Removal of the device using a water-soluble tape, 3) Completely detaching it from the skin, 4) Sterilizing the device using an alcohol swab, 5) Attaching it on the left chest, 6) Dissolution of the water-soluble tape with water.

(3M, USA) as a supporting substrate. The same device is then sterilized with a 70% isopropyl alcohol swab (Dukal, USA), and subsequently applied to the chest, where the tape is washed away, and ECG signals are acquired. We could repeat 10 cycles of removal, sterilization, and re-application of a single device without any damage, thereby enabling reuse.

The performance of a capacitive EES can be directly compared to that of a conventional Ag/AgCl electrode with conductive gel and a direct contact EES electrode by use of the Pearson correlation coefficient (r),^[20] defined as:

$$r = \frac{\sum_{i=1}^n (X_i - \bar{X})(Y_i - \bar{Y})}{\sqrt{\sum_{i=1}^n (X_i - \bar{X})^2} \sqrt{\sum_{i=1}^n (Y_i - \bar{Y})^2}}$$

where X_i , Y_i and \bar{X} , \bar{Y} denote the i^{th} sample and the mean for each data set, respectively. The capacitive EES was prepared in configurations described previously: 1 cm × 1 cm FS electrodes with 25% area coverage, a 5-μm-thick Solaris insulating

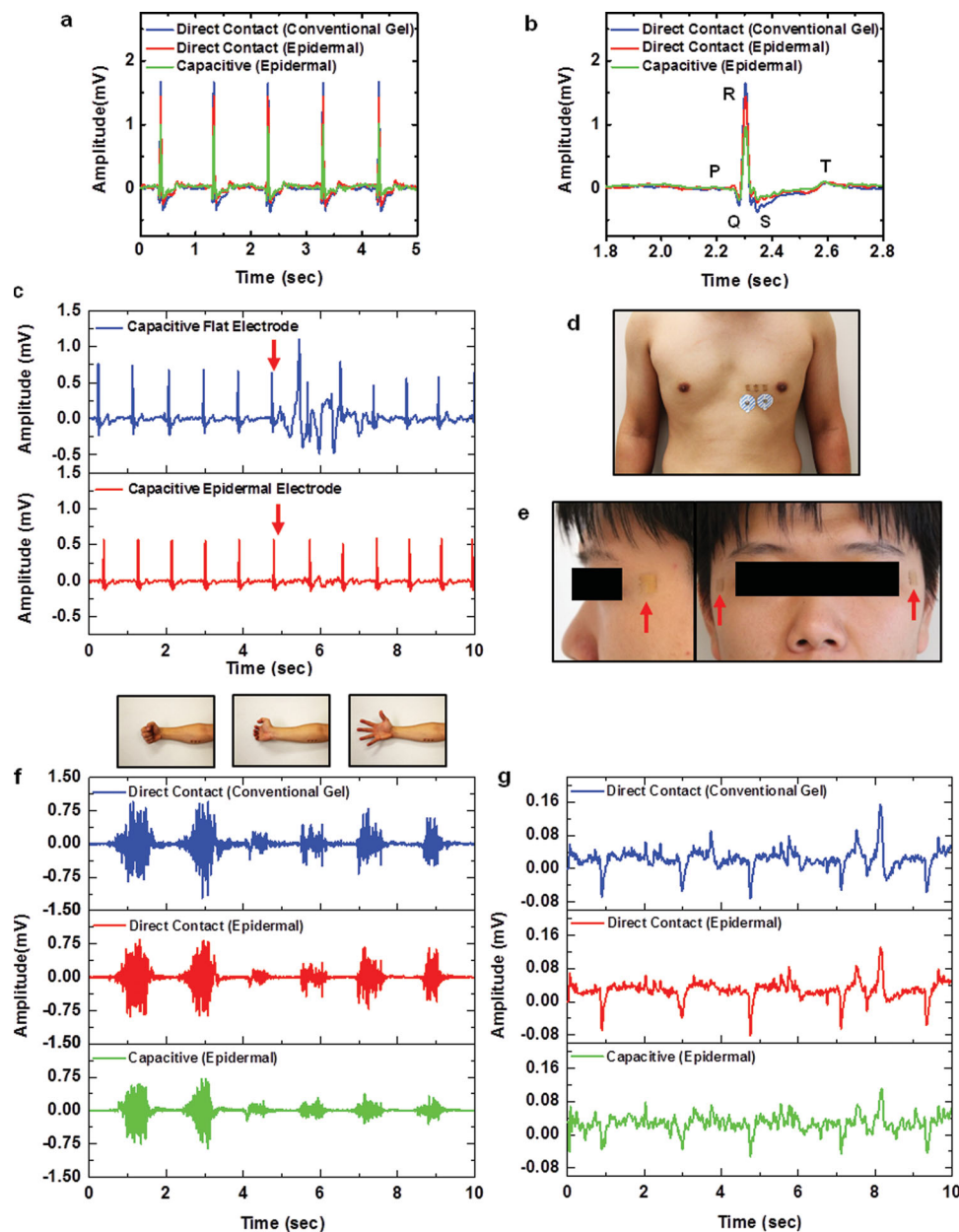


Figure 4. Applications of capacitive EES. a) Plot of ECG signals measured using standard gel electrodes with direct contact (blue), direct contact EES (red), and capacitive EES (green). b) Magnified view of an ECG signal in (a). c) Comparison of capacitive flat, rigid electrodes, and capacitive EES in terms of motion artifact in ECG signals. Red arrows indicate the point in time that the upper body moved. d) Sensor locations on the chest for ECG measurement for the experiment in (c). e) Sensor location on the face for EOG measurement. f) Plot of EMG signals measured using standard gel electrodes, direct contact EES, and capacitive EES while different hand gestures are made. g) Plot of EOG signals measured using standard gel electrodes, direct contact EES, and capacitive EES while reading a book.

layer and a 5- μm -thick Solaris substrate. The measurements involve contact of the capacitive EES, direct contact EES (same design as the capacitive EES, but without the Solaris insulating layer), and conventional gel electrodes (1 cm in diameter) on the left side of the chest for detection of ECG signals. With the capacitive EES, the P wave, the QRS complex and the T wave are clearly defined, with a quality of measurement that is comparable to that of data obtained using conventional electrodes and direct contact EES (Figure 4a,b). The ECG signals from

capacitive EES and conventional electrodes have $r \approx 98\%$, which is very close to the value ($r \approx 99\%$) for ECG signals from direct contact EES and conventional electrodes.

A major disadvantage of conventional capacitive detection is its susceptibility to artifacts caused by motion-induced variations in capacitive coupling.^[21] To minimize such effects, the electrodes must maintain robust, intimate contact with the skin during movement. Conventional capacitive sensors use rigid electrodes with small, sometimes poorly controlled, air

gaps at the electrode–body interface that can be altered by relative motions (Figure S6, Supporting Information). The thin, soft, and stretchable properties of EES enable conformal contact on the surface of the body, with the ability to accommodate skin deformation in real time. This type of coupling minimizes motion artifacts (Figure S6; interface mechanics analysis (Figure S8, Supporting Information). Measurements of sensitivity to body movement for ECG signals acquired from the chest (Figure 4d) using capacitive EES and capacitive flat, rigid electrodes highlight the differences. Both sensors use a 5- μm -thick layer of Solaris as the insulator. Securing all the cables to the body and the adjacent table ensures that any motion artifacts arise from the electrode–skin interface, and not from the cables. Figure 4c shows that the capacitive EES exhibits much less sensitivity to body motions (upper body swing) than the conventional electrode.

The same type of capacitive EES allows EMG and EOG recording. As demonstrations, EMG signals were measured on the flexor carpi radialis of the forearm during different motions of the hand and fingers (Figure 4f). The capacitive EES and conventional gel electrodes yield similar signal amplitudes and the activation timing ($r \approx 61\%$; $r \approx 80\%$ for direct contact EES and conventional gel electrodes; discrepancies arise from differences in positioning across the arm). The results indicate clear potential for use in clinics and research labs for diagnosis of neuromuscular disorders,^[22] study of muscle pain,^[23,24] and control of prosthetic and orthotic devices.^[25] In another example, EOG was recorded by placing pairs of electrodes near the left and right eye (Figure 4e,g). During the recording, the subject was asked to read a book, as a means to periodic changes associated to movement of the eyes along the lines of text. The EOG signals recorded by capacitive EES have $r \approx 81\%$ compared to those from conventional gel electrodes ($r \approx 94\%$ for EOGs measured using direct contact EES and conventional gel electrodes). The results suggest utility of capacitive EES for ophthalmological diagnosis and, more generally, for recording eye movements.

In summary, the work reported here illustrates advantages in EP measurements that follow from combined use of capacitive detection schemes and concepts of epidermal electronics. The resulting devices offer enhanced levels of wearability, expanded options in device sterilization and reuse, and minimized artifacts from body motions compared to previously reported technologies, including direct contact epidermal electrodes. The ability to completely isolate the electronics and the electrodes from the body has particular advantages in measurements on internal organs, where immersion in biofluids can otherwise create significant challenges in minimizing leakage currents.^[26] Exploring these options and integrating signal processing and wireless data transmission capabilities into the EES represents promising directions for future research. Such technology would build on advances in telemedicine and ubiquitous healthcare.

Experimental Section

Fabrication of Capacitive EES: The fabrication begins with a glass slide coated with a 10- μm -thick layer of PDMS. Exposing the PDMS to UV-induced ozone creates a hydrophilic surface for spin casting a layer

of PI (300 nm in thickness through dilution with pyrrolidinone, Sigma-Aldrich, USA). Photolithographic patterning of a bilayer of Cr (5 nm)/Au (200 nm) deposited by electron beam evaporation defines the layout of the EES. Casting another layer of PI (300 nm in thickness) locates the metal at the neutral mechanical plane (NMP). Reactive ion etching of selected regions of the PI exposes the EES electrodes and bonding pads. A water-soluble tape (3M, USA) enables retrieval of the resulting mesh structure, to expose its back surface for deposition of Ti (5 nm)/SiO₂ (80 nm) by electron beam evaporation. Transfer to a thin silicone substrate (Solaris, Smooth-On, USA) coated on a sheet of PVA (Haining Sprutop Chemical Tech, China) results in the formation of strong bonds due to condensation reactions between exposed hydroxyl groups on the SiO₂ and the silicone. Washing away the tape completes the transfer. The final step in the fabrication involves spin-casting silicone (Solaris, Smooth-On, USA) to form the insulation layer for capacitive detection.

Experiments on Human Subjects: All experiments on human skin were conducted under approval from Institutional Review Board at the University of Illinois at Urbana-Champaign (protocol number: 13229).

Supporting Information

Supporting Information is available from the Wiley Online Library or from the author.

Acknowledgements

This study was supported by the US Department of Energy, Division of Materials Sciences under Award No. DE-FG02-07ER46471 through the Materials Research Laboratory at the University of Illinois at Urbana-Champaign. J.A.R. acknowledges a National Security Science and Engineering Faculty Fellowship.

Received: August 7, 2013

Revised: September 8, 2013

Published online: October 16, 2013

- [1] Y. Yama, A. Ueno, Y. Utikawa, presented at *IEEE EMBS*, Lyon, France, August 2007.
- [2] F. Torres, M. D. Gracas, M. Melo, A. Tosti, *Clin. Cosmet. Investig. Dermatol.* **2009**, 2, 39.
- [3] E. McAdams, in *Encyclopedia of Medical Devices and Instrumentation* (Ed: J. G. Webster), John Wiley & Sons, Inc., New York 2006.
- [4] A. Potter, L. Menke, *IEEE Trans. Biomed. Eng.* **1970**, BME-17, 350.
- [5] R. N. Wolfson, M. R. Neuman, presented at *22nd ACEMB*, Chicago, USA, 1969.
- [6] S. M. Lee, J. H. Kim, H. J. Byeon, Y. Y. Choi, K.S. Park, S.-H. Lee, *J. Neural. Eng.* **2013**, 10, 1.
- [7] A. Ueno, T. Yamaguchi, T. Iida, Y. Fukuoka, Y. Uchikawa, M. Noshiro, *Sens. Mater.* **2012**, 24, 335.
- [8] R. Matthews, N. J. McDonald, P. Hervieux, P. J. Turner, M. A. Steindorf, presented at *IEEE EMBS*, Lyon, France, August 2007.
- [9] Y. M. Chi, T.-P. Jung, G. Cauwenberghs, *IEEE Rev. Biomed. Eng.* **2010**, 3, 106.
- [10] C. Metzger, E. Fleisch, J. Meyer, M. Dansachmuller, I. Graz, M. Kaltenbrunner, C. Keplinger, R. Schwodiauer, S. Bauer, *Appl. Phys. Lett.* **2008**, 92, 013506.
- [11] D. P. J. Cotton, I. M. Graz, S. P. Lacour, *IEEE Sens. J.* **2009**, 9, 2008.

- [12] S. C. B. Mannsfeld, B. C.-K. Tee, R. M. Stoltenberg, C. V. H.-H. Chen, S. Barman, B. V. O. Muir, A. N. Sokolov, C. Reese, Z. Bao, **2010**, 9, 859.
- [13] D. J. Lipomi, M. Vosgueritchian, B. C.-K. Tee, S. L. Hellstrom, J. A. Lee, C. H. Fox, Z. Bao, **2011**, 6, 788.
- [14] D.-H. Kim, N. Lu, R. Ma, Y.-S. Kim, R.-H. Kim, S. Wang, J. Wu, S. M. Won, H. Tao, A. Islam, K. J. Yu, T.-I. Kim, R. Chowdhury, M. Ying, L. Xu, M. Li, H.-J. Chung, H. Keum, M. McCormick, P. Liu, Y.-W. Zhang, F. G. Omenetto, Y. Huang, T. Coleman, J. A. Rogers, *Science* **2011**, 333, 838.
- [15] V. Arumugam, M. D. Naresh, R. Sanjeevi, *J. Biosci.* **1994**, 19, 307.
- [16] J. Lu, C. P. Wong, *IEEE Trans. Dielect. Electr. Insul.* **2008**, 15, 1322.
- [17] H. J. Baek, H. J. Lee, Y. G. Lim, K. S. Park, *IEEE Trans. Biomed. Eng.* **2012**, 59, 3422.
- [18] J.-W. Jeong, W.-H. Yeo, A. Akhtar, J. Norton, Y.-J. Kwack, S. Li, S.-Y. Jung, Y. Su, W. Lee, J. Xia, H. Cheng, Y. Huang, W.-S. Choi, T. Bretl, J. A. Rogers, *Adv. Mater.* **2013**, unpublished.
- [19] *Medical Instrumentation: Application and Design* (Ed: J. G. Webster), Houghton Mifflin, Boston **1998**.
- [20] L.-D. Liao, I.-J. Wang, S.-F. Chen, J.-Y. Chang, C.-T. Lin, *Sensors* **2011**, 11, 5819.
- [21] A. Serteyn, X. Lin, O. Amft, presented at the 4th ISABEL, Barcelona, Spain **2011**.
- [22] J. M. Gilchrist, G. M. Sachs, *Muscle Nerve* **2004**, 29, 165.
- [23] C. Bodere, S. H. Tea, M. A. Giroux-Metges, A. Woda, *Pain* **2005**, 116, 33.
- [24] D. Farina, L. Arendt-Nielsen, T. Graven-Nielsen, *Clin. Neurophysiol.* **2005**, 116, 1558.
- [25] C. Castellini, P. Smagt, *Biol. Cybern.* **2009**, 100, 35.
- [26] O. Graudejus, B. Morrison, C. Goletiani, Z. Yu, S. Wagner, *Adv. Funct. Mater.* **2012**, 22, 640.